

# Influence of Diethanolamine on Hard Segment Ordering in Flexible Polyurethane Foams

DIMITRIOS V. DOUNIS, GARTH L. WILKES

Department of Chemical Engineering, Polymer Materials and Interfaces Laboratory, Virginia Polytechnic Institute and State University, Blacksburg, Virginia 24061-0211

Received 16 August 1996; accepted 19 November 1996

**ABSTRACT:** In this study the microphase separation and structural organization of the hard segment domains were studied as a function of diethanolamine (DEOA) content for two series of model foams based on toluene diisocyanate (TDI) and glycerol initiated ethylene-oxide-capped propylene-oxide or glycerol initiated propylene-oxide. It was found that as the DEOA content was increased, the more disordered the hard segment domains became. Extractions in dimethyl formamide (DMF) showed that increasing the DEOA content increased the gel fraction, confirming that DEOA further crosslinked the system. More importantly, it was also found that the hard segment domains were also influenced by the DEOA content where the foams lacking DEOA had a much higher level of short range ordering. This was first confirmed by wide-angle x-ray scattering (WAXS) patterns where the amorphous character was much more pronounced as the DEOA content was increased. In addition, Fourier transform infrared (FTIR) data from the carbonyl region showed that the level of bidentate urea or strong hydrogen bonding also decreased as the DEOA content was increased, confirming that the short range ordering does decrease with increased DEOA content. This observation is believed to help explain the greater ease of "plasticization" by temperature and moisture observed of foams that included DEOA in their formulation. This was exemplified by comparing the load relaxation behavior at a low temperature (35°C) and a high temperature (100°C) between two foams varying in DEOA content. At ambient conditions (40°C, 35%RH), the foam with DEOA exhibited slightly higher loads at any given loading time, while at elevated conditions (100°C, 98%RH), there was very little difference between the two foams. Although the observed load relaxation behavior was mostly a result of the increased crosslinking, the increased closed cell content induced by the greater crosslinking also contributed to the load values. © 1997 John Wiley & Sons, Inc. *J Appl Polym Sci* **65**: 525–537, 1997

## INTRODUCTION

Polyurethane foams are used in a very wide range of applications, including the areas of insulation, packaging, and load-bearing, such as cushioning. Molded foams, one class of flexible polyurethane foams, are foams in which the formulation mix is either poured into a heated mold that is then closed, or injected into a closed mold. This class

of foams, a relatively newer technology, comprises an increasing fraction of polyurethane foams because they possess many advantages over slab-stock foams—the greatest being that the foam can be molded into the desired intricate shape, thereby eliminating the need for labor-intensive cutting and waste. Also, molded foams can be produced with multiple zones of hardness, with reinforcements, or with a liner such as a plastic or fabric skin, which reduce labor costs of final product assembly. The majority of molded foams are used in transportation seating and trim parts. However, they are also used in packaging, furni-

Correspondence to: Garth L. Wilkes (gwilkes@vt.edu)

© 1997 John Wiley & Sons, Inc. CCC 0021-8995/97/030525-13

ture, and novelty items. Molded foams do not differ from slabstock foams in just that they are produced in molds rather than in a semicontinuous process but, in fact, are considerably more complicated. Generally, higher-molecular-weight, more reactive polyols are used in molded foams for reasons of increased productivity. In addition to more reactive polyols, other additives such as copolymer polyols and crosslinkers are added to improve the foam's hardness and shorten demold times by enhancing the thermosetting processes. For example, diethanolamine (DEOA) is often added to increase the amount of covalent network character providing a crosslinked polymer at the time of cell-opening, which is crucial for stability of the foam. Along with a higher reactivity formulation, factors such as size of individual shot, release agents, mold temperature gradients, and curing times also contribute to the complexity.

A comparison between molded foams and slabstock foams has recently been reported by McClusky et al.<sup>1</sup> They found that the development of urea hydrogen bonding was much more distinct in slabstock foams over molded foams as observed with Fourier transform infrared (FTIR). The viscosity profiles were also very different where initial viscosity build-up was attributed to the development of bidentate urea hard segments in the slabstock foam. In the molded foam, an increase in viscosity was observed at the onset of covalent gel and did not show evidence of bidentate urea formation. These differences were attributed to the addition of DEOA and ethylene oxide capping. Furthermore, the authors developed a TDI-based molded foam with DEOA (1 pph) and a TDI-based molded foam without DEOA and followed the "real time" FTIR carbonyl development. In the foam without DEOA, a distinct bidentate peak began to develop at ~ 160 s after pouring. In contrast, the DEOA containing foams never did develop bidentate hydrogen bonding but only the disordered urea band was observed by FTIR.

The present authors also qualitatively investigated the structure-property behavior of molded foams and compared the results to those for slabstock foams.<sup>2</sup> We found that the physical properties of the molded foams were much easier "plasticized" by temperature and humidity relative to the slabstock foams. Specifically, viscoelastic and compression set properties were studied as a function of temperature and humidity for a series of molded foams and slabstock foams. It was also found that the hard segment domains in the slab-

stock foams had a much higher level of short range ordering. This was first confirmed by comparing the wide angle x-ray scattering (WAXS) patterns where it was observed that the amorphous character was much more pronounced in the molded systems of equal water/TDI content. Second, FTIR data from the carbonyl region showed that the slabstock foam had a much higher level of bidentate urea or strong hydrogen bonding within the hard segments. Conversely, the molded foam displayed no bidentate urea but only monodentate urea or very weak hydrogen bonding within the hard segments. It was concluded that the dramatic differences between the mechanical properties of molded and slabstock foams were due in part to the lower and weaker ordering of the hard segments in molded systems, making these physical crosslinks more labile at higher temperatures and humidities.

In view of this trend, the need exists for a greater fundamental understanding of the relationships between the structure/morphology and physical properties of the two types of polyurethane foams, slabstock and molded. For example, the network structure of a typical polyurethane foam is comprised of both chemical and physical crosslinks. The chemical crosslinks arise from the use of a hydroxyl polyol of functionality greater than two, while the physical crosslinks arise from the phase-separated hard segment domains (urea segments). Although both types of crosslinks enhance the foam's physical properties, the physical crosslinks are labile at high temperatures and high humidity, thus dramatically altering the foam's properties. Furthermore, the organization of these domains can strongly influence the degree of plasticization that can occur.

To help provide insight on the complicated nature of the molded foams, a series of model foams were formulated with systematically varying the DEOA content. This article correlates DEOA content to the morphology and structure of the foams, and specifically that of the HS domains utilizing two important techniques. Many authors, ourselves included, have used infrared spectroscopy in studying the morphology of polyurethane foams, and specifically the organization of the HS domains.<sup>1</sup> However, this article also incorporates another important technique, that of WAXS, which compliments and helps delineate some of the limitations of the infrared results. Thus, WAXS and FTIR were used together to ascertain the structural order of the HS domains.

**Table I Formulation Components of Foams Utilizing EO-Capped Polyols Varying in DEOA Content**

Foam	FeD-0	FeD-1	FeD-2
V4701	70.0	70.0	70.0
XAS10921	30.0	30.0	30.0
DEOA	0.0	1.0	2.0
WATER	5.0	5.0	5.0
DC-5160	1.1	1.1	1.1
DABCO	0.12	0.08	0.08
T-9	0.19	0.15	0.15
TDI	55.3	57.9	60.4

The values in the table designate the formulation amounts in terms of pph by weight of polyol. The functions of each of the chemicals listed above are as follows: V4701, 5,000 mol wt glycerol initiated ethylene oxide capped propylene oxide; DEOA, diethanol amine, a crosslinking agent; Water, blowing agent; DC-5169, a surfactant used to control and eliminate basil cells; T-9, a tin catalyst commonly known as stannous octoate; DABCO 33LV, tertiary amine primarily a blowing catalyst; TDI, a blend of isomers of toluene diisocyanate.

## EXPERIMENTAL

### Materials

In evaluating the effect of DEOA on the structure-property behavior of flexible molded polyurethane foams, two series of model polyurethane foams were formulated such that the DEOA content was systematically varied to provide trends and allow for its influence on the bulk properties to be ascertained.

The two foam systems developed from varying these components are regarded as model systems, since neither can easily be completely classified as a molded or a slabstock foam. They were formulated using a box-foaming operation, but one series incorporated ingredients typically found in molded foams such as the EO-capped 5000 mol wt polyol (V4701) while the other series utilized typical slabstock ingredients with minor modifications. The first series consisted of three foams labeled FeD-x, where "x" denotes the DEOA content in pph relative to polyol, and the "e" suggests that EO-capped polyols were used. The formulation components of each foam are listed in Table I. As can be seen, the DEOA content was varied from 0 (FeD-0) pph to 2.0 pph (FeD-2). It should also be pointed out that 2 pph DEOA is slightly beyond the amount often used (~ 1–1.5 pph) by foam formulators but was intentionally chosen here to emphasize the influences of DEOA. The

fact that 2 pph is slightly beyond the optimum amount will be made evident in this report.

As can be seen in Table I, only a very small amount by weight of DEOA is added relative to the amount of polyol. However, because of the much lower molecular weight of DEOA, the amount of functional groups supplied by the DEOA approaches the amount supplied by the polyol. For example, 2 g of the 105 mol wt DEOA molecule gives nearly the same amount of functional groups as 100 g of a 5000 mol wt molecule having the same functionality. As expected, the inclusion of DEOA has some adverse effects, such as reducing cell openness and the processing latitude requiring more extensive cell opening measures, such as adjusting the catalyst/surfactant package. Regarding the polyol, ~ 5–10% EO capping was used for the 5000 mol wt polyol, resulting in ~ 70% primary hydroxyls. Polyol V4701 is considered a rather low reactivity polyol for molded foams. As the DEOA level was increased, the tin level was slightly adjusted (decreased) accordingly, as was the toluene diisocyanate (TDI) to adjust for stoichiometric differences. For these samples, the TDI index was 103.

The second series of foams formulated with varying amounts of DEOA was made using a conventional all propylene oxide polyol, V2100. These foams are labeled as FD-x, where again "x" denotes the DEOA content, and whose value is given in Table II along with the other formulation components. Here the "e" is omitted to denote that no EO capping is present. The other components are roughly the same as those used in the FeD-x series.

**Table II Formulation Component of Foams All PO Varying in DEOA Content**

Foam	FD-0	FD-0.5	FD-1
V-2100	100.0	100.0	100.0
DEOA	0.0	0.5	1.0
WATER	5.0	5.0	5.0
DC-5160	1.2	1.2	1.2
DABCO-8264	0.12	0.12	0.12
T-9	0.23	0.23	0.25
TDI	59.0	60.3	61.5

The values in the table designate the formulation amounts in terms of pph by weight of polyol. The functions of each of the chemicals listed above are as follows: V2100, 3,000 mol wt glycerol initiated propylene oxide polyol; DEOA, diethanol amine, a crosslinking agent; Water, blowing agent; DC-5169, a surfactant used to control and eliminate basil cells; T-9, a tin catalyst commonly known as stannous octoate; DABCO 8264, tertiary amine primarily a blowing catalyst; TDI, a blend of isomers of toluene diisocyanate.

**Table III Solvent Extraction Results for EO-Capped Foams Varying in DEOA Content**

Foam	Sol Fraction (%)
FeD-0	18.5
FeD-2	6.5

**Methods**

Many techniques were used to characterize the cellular structure, morphology, and viscoelastic behavior of these foams such as scanning electron microscopy (SEM), transmission electron microscopy (TEM), dynamic mechanical analysis (DMA), small angle x-ray scattering (SAXS), WAXS, FTIR, solvent extraction, and load relaxation.

Extraction experiments were carried out on se-

lected samples to qualitatively determine the level of crosslinking and how it is influenced by specific formulation ingredients. Samples of various shape and size ( $<0.15$  g) were cut from the center of the foam bun, dried under vacuum at  $40^{\circ}\text{C}$ , and weighed. The samples were submerged in DMF ( $\sim 10\times$  by volume) for a period of 48 h. The samples were then removed from the DMF, dried under vacuum at  $40^{\circ}\text{C}$  for  $\sim 24$  h, and finally at  $80^{\circ}\text{C}$  for an additional  $\sim 48$  h. The weight of the samples was measured incrementally throughout the drying process.

The cellular structure of these foams was evaluated and compared using SEM. Thin slices (3–4 mm) of foam were first obtained using a razor blade, and were then adhered to aluminum stubs using silver paint. After  $\sim 24$  h for drying, a thin layer of gold was applied to the surface of the foam

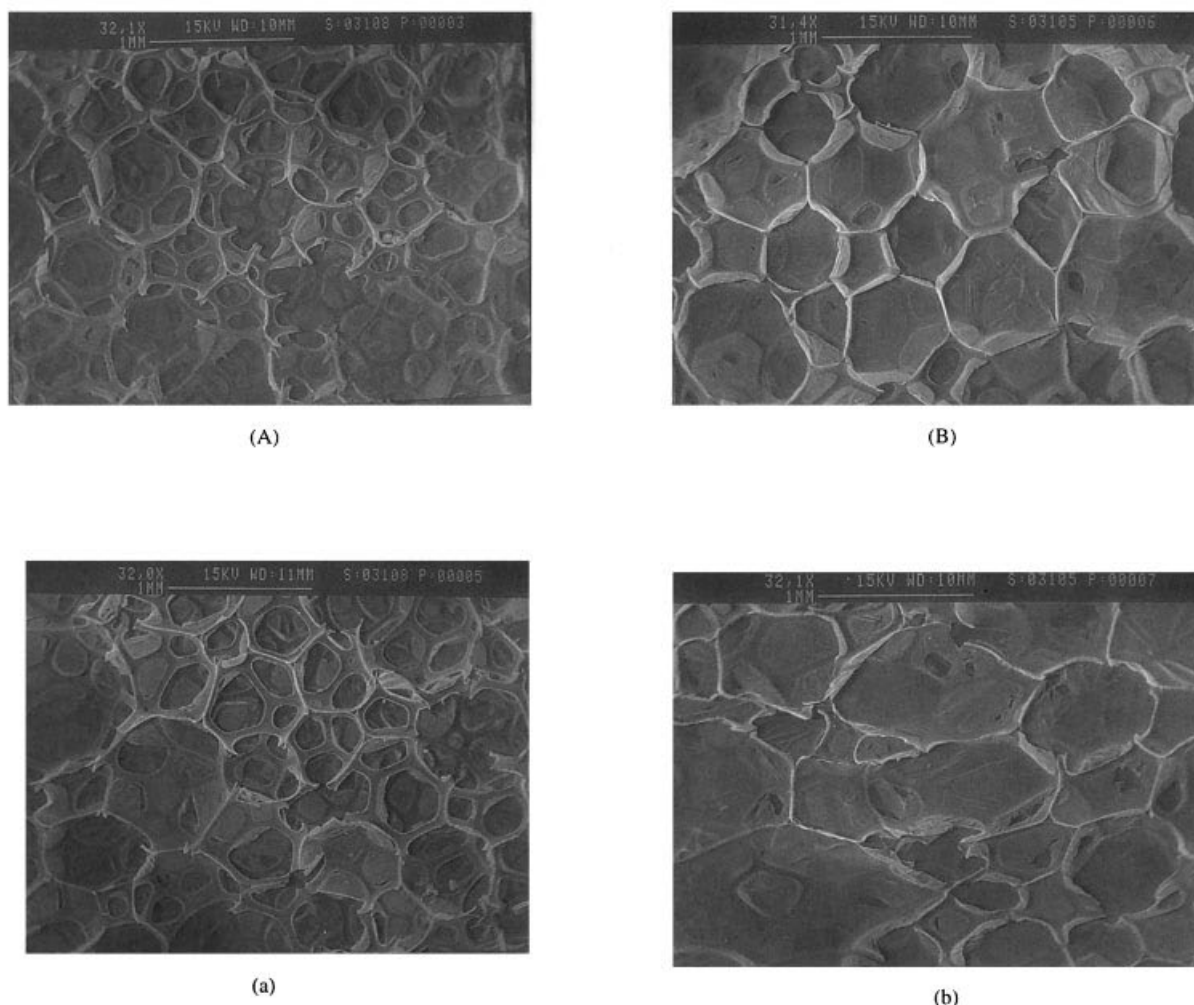
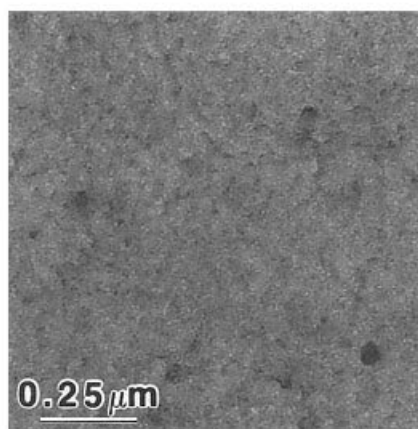
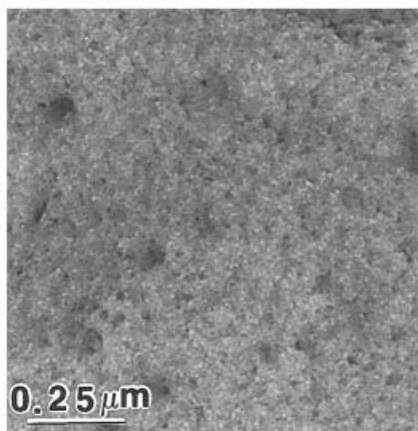


**Figure 1** Scanning electron micrographs of foam (A) FeD-0 and (B) FeD-2 shown both (a) parallel to the rise direction and (b) perpendicular to the rise direction.



(a)



(b)

**Figure 2** Transmission electron micrographs of foam (a) FeD-0 and (b) FeD-2 at a magnification of 69.6kx.

using a SPI model 13131 sputter coater. Micrographs were taken using a Cambridge model Stereoscan 100 operating at 20 kv and at a magnification of  $\sim 30\times$ . In some cases, the micrographs were obtained on a Phillips model 505.

Transmission electron microscopy (TEM) was used to ascertain the effect of DEOA on the precipitated urea-based structures, which have been reported to exist in certain slabstock foams.<sup>3</sup> The same procedure was used for both cases. Thinner samples were cut in a similar manner to those for SEM. From these samples, very thin sections were cryogenically microtomed using a diamond knife on a Reincart Junct model FC40 ultramicrotome operating at  $-90^\circ\text{C}$ . Ethanol was used to collect the sections onto 600 mesh copper grids. Some micro-

graphs were taken using a Zeiss 10CA transmission electron microscope equipped with a LaB<sub>6</sub> electron gun operating at an accelerating voltage of 80 kv. Others were taken using a scanning transmission electron microscope (STEM) operating at an accelerating voltage of 80 kv.

Dynamic mechanical analysis (DMA) was carried out using a Seiko model 210 in the tension mode. The samples were heated from  $-100^\circ\text{C}$  to  $140^\circ\text{C}$  at a rate of  $1^\circ\text{C}/\text{min}$ . from which the storage modulus ( $E'$ ) and  $\tan \delta$  data were collected at a frequency of 1 Hz. The sample dimensions were  $\sim 6.8 \times 6.8 \times 25$  mm with a grip-to-grip distance of 10 mm.

WAXS patterns were obtained using a Philips x-ray generator model PW1720, a Statton camera, and a fine focus tube with nickel-filtered CuK $\alpha$  radiation having a wavelength of 1.542 Å. Foam samples were cut  $\sim 10$  mm thick and compressed to  $\sim 3$  mm. The sample-to-film distance was 8 cm and exposure times were  $\sim 10$  h.

FTIR was used to study the hydrogen bonding within the hard segments of the foams and the relative degree of order of the hard segments in either the molded foams and slabstock foams, and how this local order is influenced by the specified formulation variables. The spectral profiles were obtained on a Digilab FTS-40 spectrophotometer equipped with an attenuated total reflectance (ATR) cell. For each sample, 64 scans were averaged, taken in the range of  $4000\text{ cm}^{-1}$  to  $400\text{ cm}^{-1}$  with a resolution of  $4\text{ cm}^{-1}$ . All scans were normalized to the absorbance of a CH stretch at  $2945\text{ cm}^{-1}$ . The regions studied were: the amide I region ( $1620\text{--}1800\text{ cm}^{-1}$ ), the N-H region ( $3100\text{--}3500\text{ cm}^{-1}$ ), and the isocyanate region ( $2200\text{--}2400\text{ cm}^{-1}$ ).

Load relaxation experiments were performed using a similar procedure to that used and described by Moreland, which was originally designed to mimic the ASTM procedure used for IFD testing.<sup>7</sup> Samples, having dimensions of  $3.5'' \times 3.5'' \times 1''$ , were cut from the foam bun using a band saw equipped with a wavy edge saw blade. Each sample was first dried under vacuum and at  $40^\circ\text{C}$  for 3.5 h to give each sample an equal level of moisture. The samples were then placed in an environmental chamber preset at the testing conditions for  $\sim 60$  min. The environmental chamber was purchased from Russells Technical Products and was equipped with a Watlow 922 microprocessor, which controls temperature in the range of  $0^\circ\text{C}\text{--}300^\circ\text{C}$  and humidity in the range of  $0\text{--}100\%$ . The chamber was fit into the Instron frame equipped

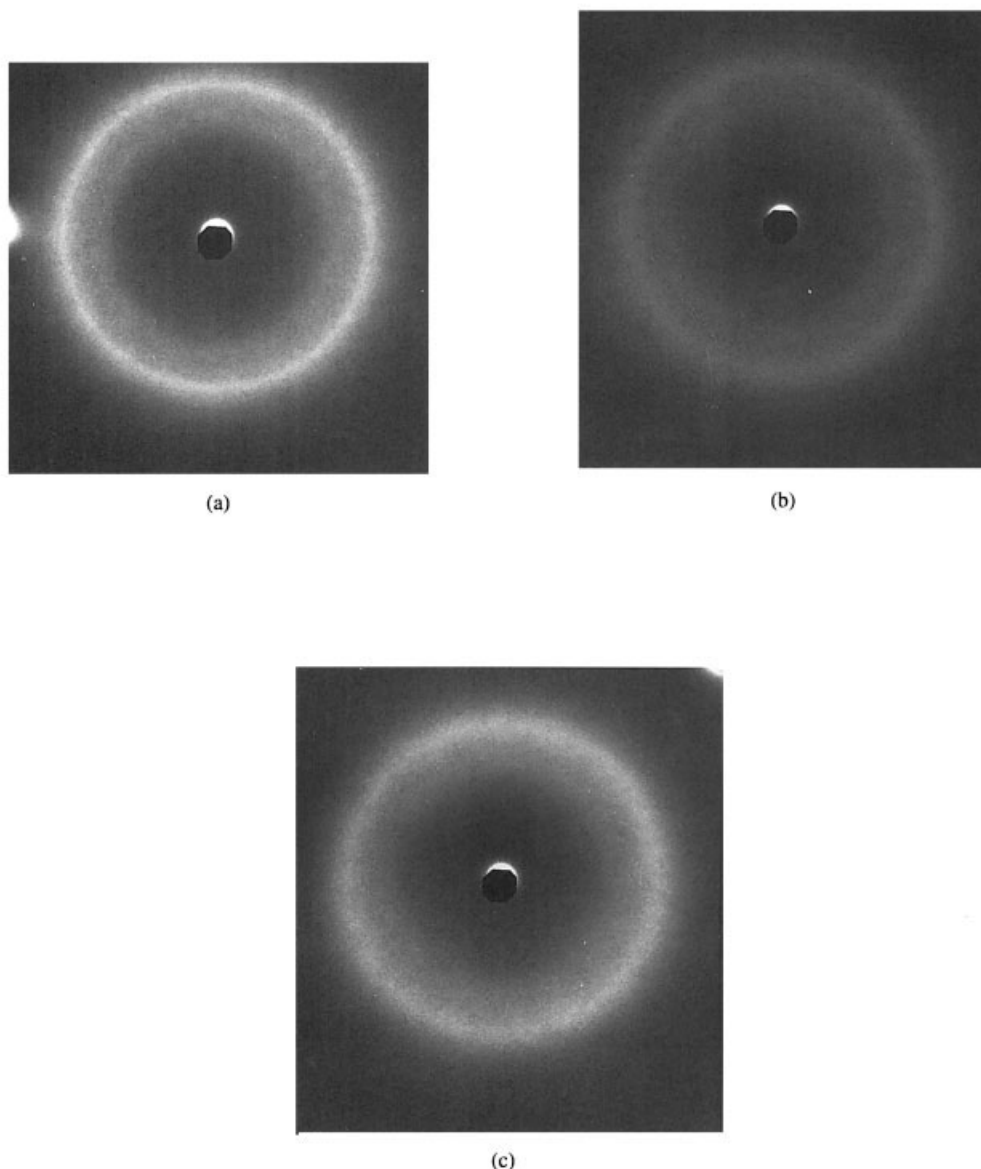


**Figure 3** WAXS patterns illustrating the influence of DEOA content on the short range ordering of the HS domains: (a) FeD-0, (b) FeD-1, and (c) FeD-2.

with a model MDB-10 compression load cell manufactured by Transducer Techniques. The load cell was positioned within an aluminum cup having a small hole through which the arm attached to the load cell can pass into the chamber, where the foam sample can rest. The cup protects the arm and thus load cell from large lateral movement, which can damage the load cell. This cup was also fitted with a line that provided a cool air purge to maintain a constant temperature due to the load cell's sensitivity to temperature. The analog signal was converted to a digital signal using a QuaTech model

ADM12-10 A/D converter from which the signal was sent to a computer.

Using a 2" indenter, initially at rest, the samples were twice compressed along the "rise Direction" to 70% and released at a rate of 350 mm/min. After 5 min the samples were compressed to 65% strain, at which point the load was immediately monitored via computer. The onset of densification for typical polyurethane foams occurs at  $\sim 65\%$  compression, above which relaxation occurs within the solid polymer independent of cellular structure.

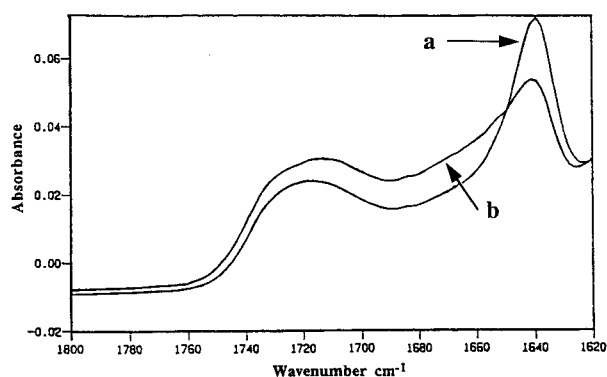


**Figure 4** Influence of DEOA content on bidentate absorbance in the FTIR spectra of foams (a) FeD-0 and (b) FeD-2.

## RESULTS AND DISCUSSION

### Characterization of Foams Made with a 5000 MW EO Capped Polyol

Solvent extractions using DMF were carried out to evaluate the amount of covalent crosslinking as a function of DEOA content, and thereby verify that DEOA does significantly influence the covalent network. Table III presents the results of this treatment, which clearly show that the amount of covalent crosslinking was increased with increasing DEOA content. The amount of extractables decreased from 18.5% for FeD-0 to 6.5% for FeD-2.

The cellular structure of the foams was studied using SEM and, indirectly, using airflow measurements. The cellular structure of foam FeD-0 is shown in Figure 1(a), which shows a typical structure of a flexible slabstock polyurethane foam containing predominantly open cells of uniform size. Recall that the "e" denotes ethylene oxide, which endcaps the propylene oxide polyol.

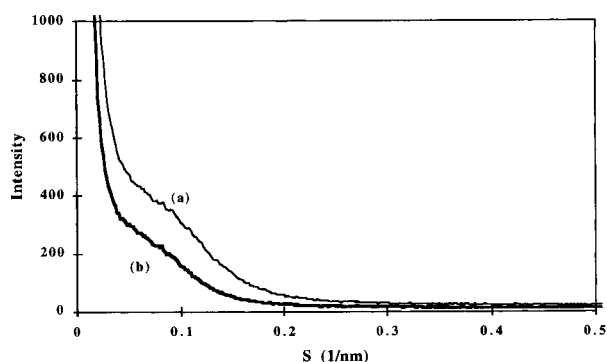


**Figure 5** SAXS profiles of (a) FeD-0 and (b) FeD-2 illustrating the influence of the DEOA content on the microphase separation.

**Table IV** Solvent Results for All PO Foams Varying in DEOA Content

Foam	Sol Fraction (%)
FD-0	7.8
FD-0.5	5.7
FD-1	3.2

With the exception of a few closed windows, the foam appears to be an open-celled foam. Comparing this foam to foam FeD-2, shown in Figure 1(b), reveals that the 2 pph DEOA content added resulted in an extremely high number of closed windows. Airflow measurements that were carried out also reflected this. While the airflow measurement of foam FeD-0 was  $\sim 5.0$  ft<sup>3</sup>/min, the airflow of foam FeD-2 was only  $\sim 0.4$  ft<sup>3</sup>/min. The latter being much lower suggests that indeed many more cell windows are still intact in this foam. The closed and larger cells are a consequence of crosslinking occurring prematurely before maximum bubble growth, which prevents the rupture of the cells. The additional crosslinking provided by the DEOA overstabilizes the cell walls, thus preventing rupture when growing bubbles impinge. The observed differences in the cellular structure of the foams as a function of DEOA content are actually differences induced in the solid structure of the foams. The solvent extraction results further verified that the resultant cellular structure is principally a consequence of enhancing the covalent network through DEOA addition.

An investigation of the fine scale structure was also carried out by TEM to determine if any urea aggregate structures could be observed that have been noted in high water-content slabstock foams.<sup>3</sup> In an attempt to determine whether DEOA had any influence on the fine structure of these foams, transmission electron micrographs were taken of the foams in this series and are presented in Figure 2(a,b) where micrograph (a) shows the structure of FeD-0 at a magnification of 69.6Kx and micrograph (b) shows the structure of FeD-2 at the same magnification. As can be seen, both micrographs show a similar texture with essentially no differences between them. Both exhibit a "grainy" texture with 100- to 150-Å dark regions with no distinct signs of any larger scale aggregate structure on the scale length of 0.1–0.5  $\mu$ m that have been noted in polypropylene oxide slabstock foams of similar water content.<sup>3</sup>

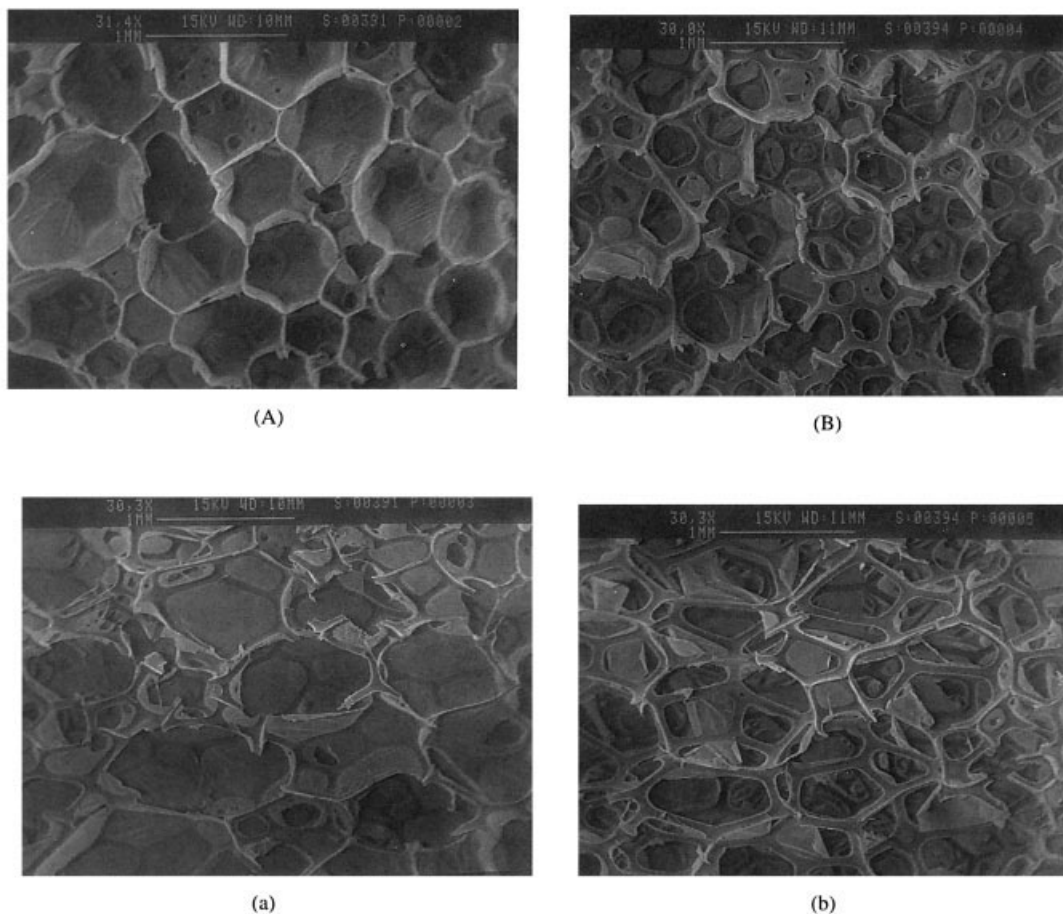


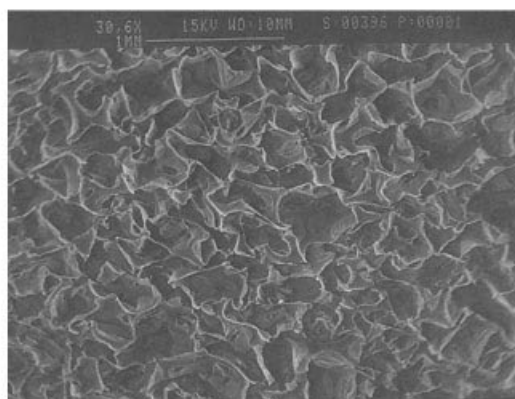
**Figure 6** Scanning electron micrographs of foam (A) FD-0, (B) FD-0.5, and (C) FD-1 shown both (a) parallel to the rise direction and (b) perpendicular to the rise direction.

The microphase separation as a function of DEOA content was evaluated in view of the well-documented influence of crosslinking affecting the phase behavior of segmented materials, in general, higher crosslinking promotes phase mixing.<sup>4,5</sup> Furthermore, the extent or perfection of phase separation has been shown to strongly influence the physical properties of the foams, especially at elevated temperatures. As mentioned earlier, both WAXS and FTIR were used to address the perfection of the HS domains. Figure 3 illustrates the WAXS patterns of foams FeD-0, FeD-1, and FeD-2. As can be seen, along with a broad amorphous halo which is typical of liquid-like amorphous systems, each pattern shows the presence of one "outer" relatively strong ring and one weaker-intensity inner ring, which are indicative of short range or paracrystalline ordering. These rings are identical in position to the WAXS patterns obtained on conventional slabstock foams such as those studied by Armistead and

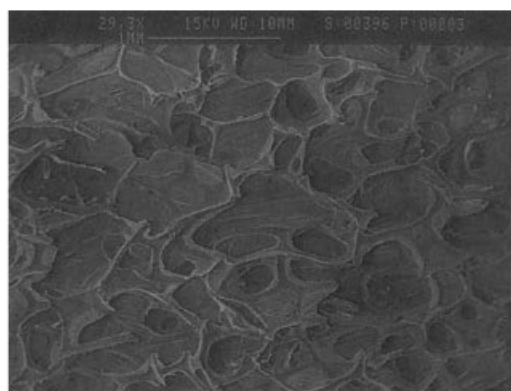
Tyagi, who have also attributed these peaks to short range order arising from the ordered hard segment within the urea hard segment domains.<sup>3,6</sup> The distinctness of the peaks indicates some degree of order, not just a maxima in the amorphous halos. Also distinctly evident in Figure 3 is that the sharpness of these rings decreases as the DEOA content is increased, clearly suggesting that the hard segment ordering is also decreasing. This evidence suggests that while DEOA increases the level of crosslinking, it also disrupts the hard segment ordering. Restated, the increased number of crosslinks restrict the process of molecular packing of the hard segments, thereby limiting the cohesiveness of the hard segment domains. In end-use applications, such decreased order can allow for the easier "plasticization" by heat and humidity, thereby making these domains more labile at these elevated conditions.

To further support the WAXS results, FTIR was carried out, which also showed that the in-





(C)



(c)

**Figure 6** (Continued from the previous page)

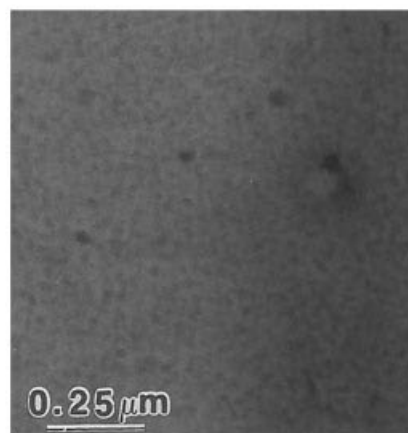
fluence of DEOA on the structural order of the HS domains was one of a disrupting nature. The FTIR spectral profiles of foams FeD-0 and FeD-2 are shown in Figure 4, which display absorbances in the carbonyl region. Evident here is that the well ordered bidentate absorbance centered at  $1640\text{ cm}^{-1}$  decreased significantly by the inclusion of 2 pph DEOA. Again, this strongly supports the evidence acquired in the WAXS analysis that DEOA does prevent the packing perfection of the HS domains or physical crosslinks.

In view of the presented results, which reveal that the HS domain packing order is disrupted with the addition of DEOA, one might assume that considerable phase mixing may be occurring or that these systems are completely phase-mixed. To verify that the foams display microphase separation on the scale of  $\sim 100\text{ \AA}$ , SAXS was carried out on the foams and the results are presented in Figure 5. As can be seen, the presence of a shoulder at the typical Bragg spacing of  $\sim 100\text{ \AA}$  clearly suggests that both the foam with

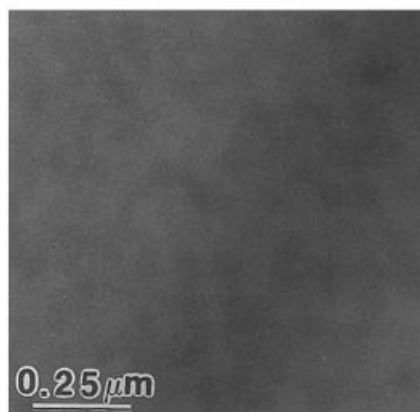
no DEOA (FeD-0) as well as the foam with the maximum amount of DEOA (FeD-2) systems display nearly identical microphase separation (as denoted by the shoulder in the SAXS profiles) although the small difference in the scattered intensity may be a result of some difference in the extent of phase separation.

#### Characterization of Foams Made with a 3000 MW All PO Polyol

As mentioned earlier, the two series of foams produced for this study differed in the type of polyol used. While the first series, which was just discussed, consisted of a 5000 mol wt EO-capped po-



(a)



(b)

**Figure 7** Transmission electron micrographs of foam (a) FD-0 and (b) FD-0.5 at a magnification of 54kx.

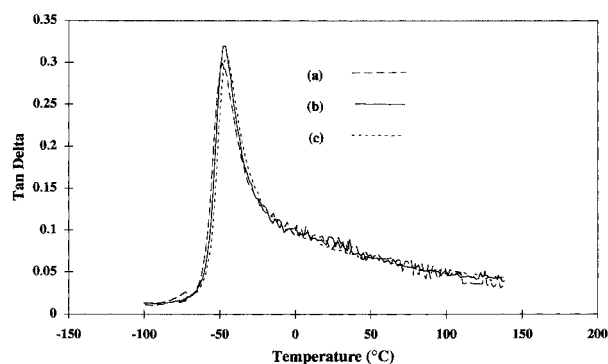


**Figure 8** Influence of DEOA content on the tan delta peak of foams (a) FD-0, (b) FD-0.5, and (c) FD-1.

lyol comparable to what might be used for a molded foam, the second series utilized a 3000 mol wt PO triol, which provided all secondary hydroxyls, as is common for conventional slabstock foams. This second series allows for the evaluation of DEOA irrespective of the effects of the EO capping. Furthermore, qualitative evaluation of the effects of the EO capping can be obtained by comparing general features of each series of foams. Again, the investigation began with solvent extractions and SEM/airflow measurements to evaluate the influence of DEOA content on covalent content and the cellular structure.

Table IV presents the results of the extraction treatment, which confirm that the amount of covalent crosslinking is again distinctly increased with increasing DEOA content. The amount of extractables decreased from 7.8% for FD-0 to 5.7% for FD-0.5, to only 3.2% for FD-1.5. Clearly, the amount of material covalently bonded within the system was again increased with increasing DEOA, as was the case for the earlier series.

The cellular structure of foam FD-0 is shown in Figure 6(a) both parallel and perpendicular to the rise direction depicting the usual geometric anisotropy when viewed perpendicular to the rise direction. As can be seen, this foam has an unusually large number of closed windows. This is likely a result of the relatively high amount of gelling catalyst used, which resulted in a somewhat improper balance between blowing and gelling, and ultimately a greater number of closed cells. Comparing these micrographs to those of foam FD-0.5, shown in Figure 6(b), also reveals a relatively high amount of closed windows. Again, the geometric anisotropy is clearly evident. Based on the micrographs, both foams appear similar in cell-

openness and size. The airflow data, however, suggest otherwise. The measured airflow of FD-0 was  $\sim 5.0 \text{ ft}^3/\text{min}$  and that of FD-0.5 was only  $0.2 \text{ ft}^3/\text{min}$ , suggesting that the continuous flow of air through the foam is greatly hindered, and thus FD-0.5 has considerably many more closed windows. In the case where the DEOA content was increased to 1.0 pph, the result was severe foam shrinkage due to the cooling, and thus contraction, of the entrapped gas within the closed cells whose cell window membranes have significantly increased in strength by the additional DEOA. The resultant cellular structure is shown in Figure 6(c), which clearly shows a severely altered structure. Although the foams still display a geometric anisotropy, the cells do not display the usual polyhedron cellular structure typical of conventional slabstock polyurethane foams.

TEM was also carried out to observe the presence of any influences on the fine structure of these foams as a function of DEOA content. In addition, based on reports<sup>3,7</sup> of the presence of what are referred to as urea precipitates or aggregate structures in "all PO high water content foams," it was desired to determine whether these structures would be observed in this series of foams, and furthermore whether DEOA had any influence on them.

The TEM of foam FD-0 is presented in Figure 7(a) and that of FD-0.5 is shown in Figure 7(b). Both micrographs display the appearance of large electron-dense regions unlike those exhibited by either of the EO capped foams, FeD-0 or FeD-2, which were shown earlier in Figure 2(a,b). The dark regions in Figure 7(a,b) range in size from 100 to 150 nm and are speculated to be urea-rich precipitates or urea aggregates in a more continu-

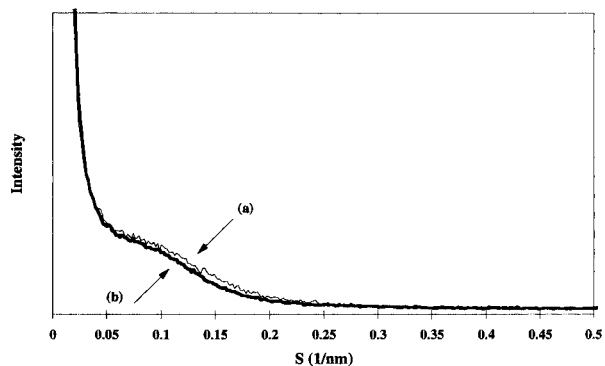


**Figure 9** SAXS profiles of (a) FD-0 and (b) FD-2 illustrating the influence of the DEOA content on the microphase separation.

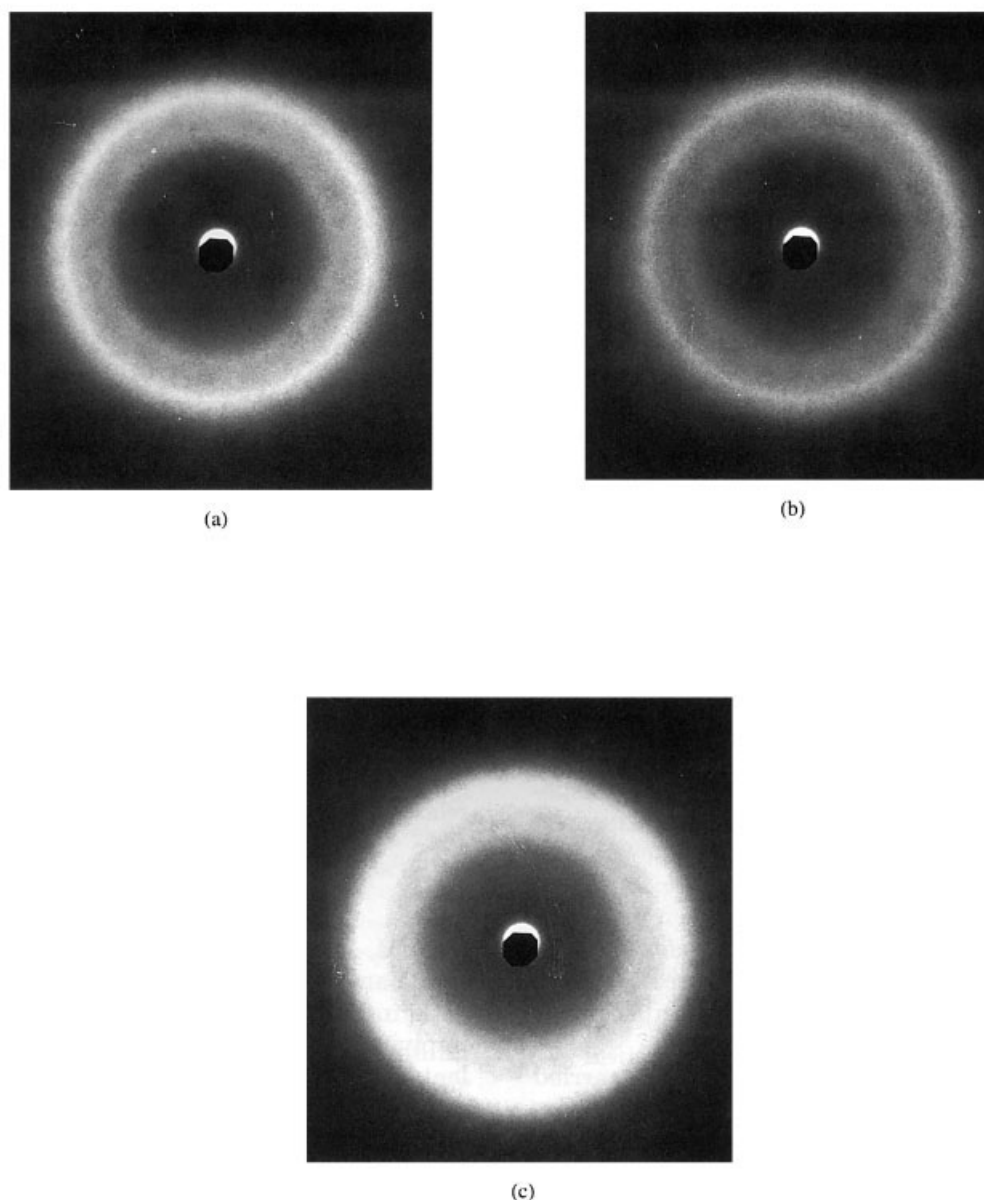


**Figure 10** WAXS patterns illustrating the influence of DEOA content on the short range ordering of the HS domains: (a) FD-0, (b) FD-0.5, and (c) FD-1.

ous softer phase comprised of soft polyol segment, along with microphase-separated hard segment domains, as will be addressed below. These larger structures are believed to be the same structures that have been observed by others in conventional higher water slabstock foams.<sup>3,7</sup> Upon comparing the micrograph of FD-0 to that of FD-0.5, it appears that the urea aggregates are more discrete with higher contrast in foam FD-0, where as in FD-0.5 they appear somewhat gray and slightly larger. This may be a result of this area consisting of a more mixed morphology of hard and soft segment components.

It was shown that DEOA distinctly influenced the HS organization within the FeD-x series discussed earlier. The effect of DEOA on the structural order of the “all PO” polyol-based system was ascertained also utilizing WAXS. In addition, dynamic mechanical analysis (DMA) was applied to determine the soft segment  $T_g$  as a function of DEOA content with the intention to qualitatively relate it to the level of phase separation. The tan delta curves of the three foams FD-0, FD-0.5, and FD-1 are shown in Figure 8. Here, the  $T_g$  of the soft segment only slightly increased with increasing DEOA content from  $-48^\circ\text{C}$  for FD-0 to  $-45^\circ\text{C}$

for FD-1. Although subtle, the results indicate that the soft segment  $T_g$  is increased a small amount due to more hard segments being “locked” within the soft segment phase. This latter statement is certainly not intended to claim that the system is well phase-mixed since the associated SAXS profiles, shown in Figure 9, clearly indicate a microphase separated morphology due to the occurrence of a broad first-order interference shoulder in the profile.

As was the case for the earlier SAXS profiles in Figure 5, the profiles in Figure 9 also suggest a correlation length of  $\sim 100 \text{ \AA}$  as based on a “Bragg law” estimation. WAXS was carried out to address the short range ordering and the influence of DEOA content on the local packing order of the hard segments within this second series of foams. Figure 10(a–c) illustrates the WAXS patterns of the foams FD-0 and FD-0.5, and FD-1. Again, in addition to the amorphous halo, two relatively sharp rings (indicating localized packing order) are displayed. As with the previous series of foams, increasing the DEOA content disrupted the ordering of the HS domains, as denoted by the subtle decrease in ring sharpness, especially with FD-1. The sharp rings displayed by FD-0 shown in Figure 10(a) have become slightly more diffuse for FD-0.5, as shown in Figure 10(b), and even more diffuse for FD-1, shown in Figure 10(c). Certainly, this evidence confirms the earlier results that while DEOA increases the level of crosslinking, it also disrupts the hard segment ordering.

Load relaxation measurements were carried out to evaluate the influence of DEOA on the viscoelastic nature of the foams. We have extensively used this technique within earlier studies to address both the viscoelastic response of the covalent network and physical network of the foams.<sup>2,4,7</sup> The relaxation results for the two “all PO” foams varying in DEOA content carried out at 30°C, 35%RH are shown in Figure 11(A), which reveals that DEOA does enhance the loads, particularly at ambient conditions. The initial loads were increased by  $\sim 20\%$  at 30°C, 35%RH with the inclusion of 0.5 pph DEOA in the formulation. It must also be pointed out that the different cellular structures exhibited by these two foams as witnessed by the airflow measurements may also influence the load relaxation behavior. For example, the increased crosslinking, in addition to strengthening the struts, produced more closed windows, which greatly reduced the airflow, further increasing the load levels. At 100°C,

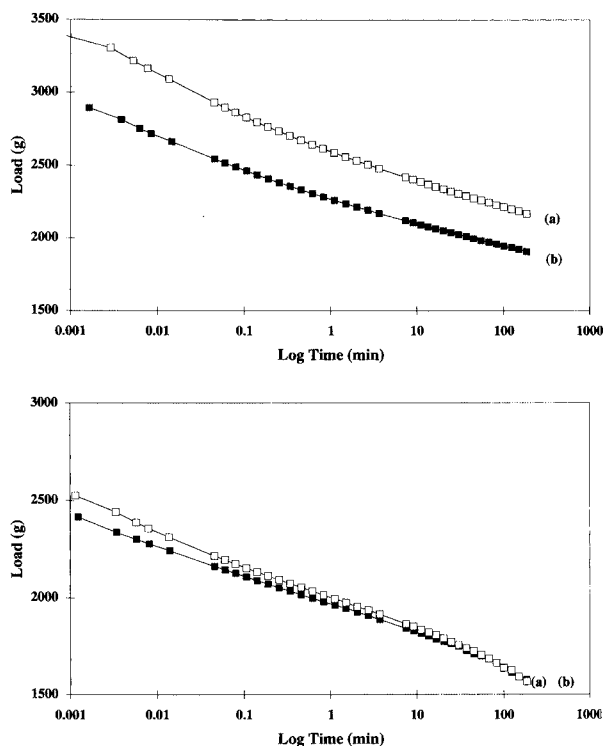


**Figure 11** Influence of the DEOA content on the load relaxation behavior at (A) 30°C-35%RH, and (B) 100°C-98%RH. In each figure the letters designate: (a) FeD-0 and (b) FeD-2.

98%RH, however, [shown in Figure 11(B)] the small amount of DEOA in the formulation had little influence on the relaxation behavior, again implying that while the DEOA increases the covalent crosslinking it also greatly “loosens” the cohesiveness of the HS domains for which moisture and temperature can easily disrupt their poorly ordered hydrogen bonding even further than in FD-0. These latter results, presented in Figure 11(B), are strong evidence, suggesting that the differences observed in Figure 11(A) are not solely due to differences in the cell-openness. Here, it is clear that the decreased cohesiveness of the HS domains does override the increased covalent crosslinking in terms of the exhibited load relaxation behavior.

## CONCLUSIONS

DEOA, an important ingredient commonly incorporated in molded foams, was evaluated by systematically varying its concentration and making the appropriate measurements to evaluate its influence on the structure and morphology of the

foams—specifically the hard segment domains. Solvent extraction results confirmed that as the DEOA was increased, the amount of covalent crosslinking also increased. However, the increased crosslinking also promoted many closed cells, which can dramatically alter the mechanical properties and even cause shrinkage of the foam pad as it cools following processing. High levels of DEOA also appeared to disrupt the larger scale urea aggregates observed with TEM for the all propylene oxide polyol-based foams. These aggregates exhibited a rather mixed morphology for the high DEOA content foams, and this is attributed to the prevention of the full development of these structures by the added DEOA earlier-induced covalent network during foam development.

The single most important discovery was with respect to the internal ordering of the HS domains—an important factor greatly influencing a foam's physical properties. The higher covalent crosslinking provided by increasing the DEOA content also severely restricted the hard segment ordering confirmed by both WAXS and FTIR. The sharpness of the rings in the WAXS patterns significantly decreased as the DEOA content was increased. In addition, FTIR illustrated that the bidentate urea absorbance also decreased as the DEOA content was increased. Thereby, the inclusion of DEOA results in the HS domains to be more labile at an elevated temperature and humidity, thereby diminishing the foam's performance.

Comparing those foams with relatively similar cellular structures demonstrated that increasing

the DEOA content increased the displayed load in load relaxation measurements at room temperatures. At elevated temperatures, however, no significant difference was observed as a function of DEOA content. This was attributed to a balance between the “tightening” of the covalent network and a “loosening” of the physical network (HS domains) as the DEOA content was increased.

The authors wish to acknowledge the Dow Chemical Co. for their financial support and for furnishing the foam samples. Professor Eva Marand is also acknowledged for the use of the Bio-Rad FTIR equipment.

## REFERENCES

1. J. V. McClusky, R. D. Priester, Jr., W. R. Willkomm, M. A. Capel, and M. D. Heaney, *Polyurethanes World Congress 1993*, 507 (1993).
2. D. V. Dounis and G. L. Wilkes, *36TH Annual Polyurethane Technical/Marketing Conference*, 507 (1995).
3. J. P. Armistead, G. L. Wilkes and R. Turner, *J. Appl. Poly. Sci.*, **33**, 801 (1988).
4. D. V. Dounis and G. L. Wilkes, *J. Appl. Poly. Sci.* in press.
5. O. Thomas, R. D. Priester, Jr., K. J. Hinze, and D. D. Latham, *J. Polym. Sci., Polym.-Phys.*, **32**, 2155 (1994).
6. D. Tyagi, Ph.D. Thesis, Virginia Polytechnic Institute and State University, Chem. Eng. Dept., Blacksburg, Virginia, 1985.
7. J. C. Moreland, Ph.D. Thesis, Virginia Polytechnic Institute and State University, Chem. Eng. Dept., Blacksburg, Virginia, 1991.